Orexin-neuromodulated cerebellar circuit controls redistribution of arterial blood flows for defense behavior in rabbits

Naoko Nisimaru[a,b], Chetan Mittal[a,c,1], Yoshinori Shirai[a,d], Thongchai Sooksawate[e,2], Prabu Anandaraj[a,c,1], Tsutomu Hashikawa[a], Soichi Nagao[a], Akiko Arata[a,f], Takeshi Sakurai[g], Miyuki Yamamoto[h], and Masao Ito[a,3]

[a]RIKEN Brain Science Institute, 2-1 Hirosawa, Wako, Saitama 351-0198, Japan; [b]Department of Physiology, Faculty of Medicine, Oita University,1-1 Idaigaoka, Hasama,Yufu, Oita 879-5593, Japan; [c]Indian Institute of Technology, Kharagpur 721-302, India; [d]Department of Neuroplasticity, Shinshu University Graduate School of Medicine, 3-1-1 Asahi, Matsumoto, Nagano 390-8621, Japan; [e]Department of Physiology, Faculty of Pharmaceutical Science, Chulalongkorn University, Bangkok 10330, Thailand; [f]Department of Physiology, Hyogo College of Medicine, 1-1 Mukogawa, Nishinomiya, Hyogo 663-8501, Japan; [g]Department of Molecular Neuroscience and Integrative Physiology, Faculty of Medicine, Kanazawa University, Kanazawa, Ishikawa 920-8640, Japan; and [h]Comprehensive Human Studies, University of Tsukuba, 1-1 Tennodai, Tsukuba, Ibaraki 305-8575, Japan

This contribution is part of the special series of Inaugural Articles by members of the National Academy of Sciences elected in 2007.

Contributed by Masao Ito, July 9, 2013 (sent for review April 27, 2012)

We investigated a unique microzone of the cerebellum located in folium-p (fp) of rabbit flocculus. In fp, Purkinje cells were potently excited by stimulation of the hypothalamus or mesencephalic periaqueductal gray, which induced defense reactions. Using multiple neuroscience techniques, we determined that this excitation was mediated via beaded axons of orexinergic hypothalamic neurons passing collaterals through the mesencephalic periaqueductal gray. Axonal tracing studies using DiI and biotinylated dextran amine evidenced the projection of fp Purkinje cells to the ventrolateral corner of the ipsilateral parabrachial nucleus (PBN). Because, in defense reactions, arterial blood flow has been known to redistribute from visceral organs to active muscles, we hypothesized that, via PBN, fp adaptively controls arterial blood flow redistribution under orexin-mediated neuromodulation that could occur in defense behavior. This hypothesis was supported by our finding that climbing fiber signals to fp Purkinje cells were elicited by stimulation of the aortic nerve, a high arterial blood pressure, or a high potassium concentration in muscles, all implying errors in the control of arterial blood flow. We further examined the arterial blood flow redistribution elicited by electric foot shock stimuli in awake, behaving rabbits. We found that systemic administration of an orexin antagonist attenuated the redistribution and that lesioning of fp caused an imbalance in the redistribution between active muscles and visceral organs. Lesioning of fp also diminished foot shock-induced increases in the mean arterial blood pressure. These results collectively support the hypothesis that the fp microcomplex adaptively controls defense reactions under orexin-mediated neuromodulation.

somatosympathetic | vestibulosympathetic | OX-1R antagonist | bicuculline | baroreceptor

The cerebellar cortex consists of numerous microzones, each extending 10 mm^2 or so (ref. 1; for review, see ref. 2). Each microzone receives three distinct types of input, that is, mossy fibers, climbing fibers, and beaded fibers. Beaded fibers contain certain amines or neuropeptides (for review, see refs. 3 and 4) and distribute diffusely; supposedly, they determine the general activity or the mode of operation of their target neurons, that is, neuromodulation, unlike input/output-specific transmission in mossy fibers and climbing fibers (5). Several microzones have been analyzed with regard to their circuit mechanisms and specific reflex functions (not only somatic; some are autonomic) (6, 7), but the actual roles of beaded fibers remain largely unknown. In this study, we focused on a particular microzone located in the flocculus [folium-p (fp)] (8, 9), which receives beaded fibers containing orexins (hypocretins) (10). Orexins consist of A and B isopeptides containing 33 and 28 amino acids, respectively, and have been implicated in sleep and feeding (11–13).

A functionally unique feature of fp is that a large portion of Purkinje cells in it are excited by stimulation of the classic defense areas in the hypothalamus and mesencephalic periaqueductal gray (PAG) (14). Electrical or chemical stimulation of the defense areas induces complex motor activities for "fight or flight" and associated cardiovascular responses such as rapid increase of blood pressure (BP) (15–17). In natural behaving conditions, harmful stimuli activate the defense areas via the amygdala (for review, see ref. 18). Involvement of orexins in the cardiovascular defense reactions has been suggested because the genetically induced orexin deficiency in mice leads to attenuation of the transient increase of blood pressure evoked from defense areas (19, 20).

We analyzed neuronal circuit connections to and from fp using axonal transport tracers. Importantly, we found that Pukinje cells in fp project their axons to the ventrolateral corner of the ipsilateral parabrachial nucleus (PBN), a major cardiovascular center in the brainstem (21, 22). It was previously shown that PBN receives Purkinje cell axons from the anterior vermis (21) as well as the middle (6) and lateralmost regions (7) of the nodulus-uvula. These observations suggest that PBN acts as a functional interface between the cerebellum and supraspinal cardiovascular centers (21). In defense reactions, arterial blood flow is redistributed from visceral organs and resting muscles to active muscles (17) by the action of the sympathetic nervous system (23). Subtle control of this redistribution is needed to maintain cardiovascular homeostasis while fulfilling the high demand for arterial blood supply to muscles actively involved in defense reactions.

On the above-introduced backgrounds, we attempted to define the role of orexins in fp function and the role of fp in the control of arterial blood flow. We used rabbits because their flocculus has discernible regular folial divisions (8, 9), which is not the case in rats or mice.

A preliminary report of this work was delivered by N.N. and M.I. at the 35th International Congress of Physiological Sciences, March 31–April 5, 2005, San Diego, CA, abstract 512.

Author contributions: N.N., A.A., M.Y., and M.I. designed research; N.N., C.M., Y.S., T. Sooksawate, P.A., T.H., S.N., A.A., M.Y., and M.I. performed research; T. Sakurai contributed new reagents/analytic tools; N.N., C.M., Y.S., T. Sooksawate, A.A., M.Y., and M.I. analyzed data; and N.N., T. Sakurai, and M.I. wrote the paper.

The authors declare no conflict of interest.

Freely available online through the PNAS open access option.

[1]On leave from: Indian Institute of Technology, Kharagpur 721-302, India.

[2]On leave from: Chulalongkorn University, Bangkok 10330, Thailand.

[3]To whom correspondence should be addressed. E-mail: masao@brain.riken.jp.

This article contains supporting information online at www.pnas.org/lookup/suppl/doi:10.1073/pnas.1312804110/-/DCSupplemental.

Results

Orexin-Immunopositive Beaded Fibers in Rabbit Cerebellum. In rabbits, the flocculus lies in the rostroventrolateral corner of the cerebellum (Fig. 1*A*) and consists of six folia, fm, f1, f2, f3, f4, and fp (8. 9) (Fig. 1*B*). In coronal sections, a cut face of fp can be identified by its flattened triangular appearance, with the peak pointing ventrolaterally (Fig. 1*C*). As examined in three complete sets of serial coronal sections (60 μm thick) of the left flocculus, the Purkinje cell layer in fp maximally expands dorsoventrally by 3.0 ± 0.1 mm (mean ± SE of mean, throughout this article) and anteroposteriorly by 3.1 ± 0.2 mm, the total area being 7.2 ± 0.9 mm^2.

Immunohistochemical data on orexins are abundant in the literature for mice and rats but are scarce for rabbits; therefore, we collected our own data for confirmation. Within the cerebellum, we observed orexin-immunopositive fibers located almost exclusively in the flocculus, with a rare detection of such fibers in the vermis, as similarly observed in rats (10). A fluorescence microscopy image shows the beaded appearance of these fibers, which lie adjacent to Purkinje cells and ascend to the molecular layer, some running parallel to the Purkinje cell layer (Fig. 2 *A* and *B*). In one flocculus, we counted 46 such fibers in the molecular layer, 74 in the Purkinje cell layer, and 71 in the granular layer. As summarized for three rabbits (Table S1), the density of orexin-immunopositive fibers in cross-sectional areas of fp is 2.77 times as high as that in all other (non-fp) folia of the flocculus. The common presence of orexin-immunopositive fibers may justify our classification of fp as part of the rabbit flocculus whereas Tan et al. (9) deemed fp as part of the ventral paraflocculus.

Origin of Orexin-Immunopositive Fibers. Within the rabbit hypothalamus, orexin-immunopositive neurons distribute around the fornix over the perifornical nucleus, dorsomedial hypothalamus, and lateral hypothalamic area (Fig. S1*A*). As similarly observed in rats (10), orexin-immunopositive axons of these cells innervate a number of structures in the brainstem and densely fill PAG (Fig. S1*C*). Orexin B-conjugated saporin (SAP, a ribosome-inactivating protein) has been used to degenerate neurons that had orexin receptor-2 (OX-2R), including orexin-immunopositive neurons; however, SAP actually degenerated not only these neurons, but also most of the other neurons in the posterior hypothalamus (24). Therefore, we injected SAP into the hypothalamus as a nonspecific lesioning agent. In two rabbits in which SAP-induced lesions covered the hypothalamus defense area bilaterally (except for some surviving orexin-immunopositive neurons) (Fig. S1*B*), orexin-immunopositive fibers in PAG largely diminished (Fig. S1*D*); this finding confirms that these fibers are branches of orexin-immunopositive fibers of hypothalamic origin.

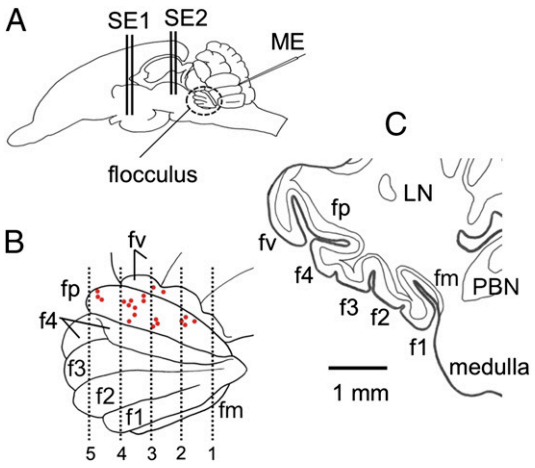

Fig. 1. Folium-p of rabbit flocculus. (*A*) Left side view of rabbit brain. ME, glass microelectrode; SE1, stimulating needle electrode inserted in the hypothalamus; SE2, another electrode in PAG. (*B*) Enlarged left side view of the flocculus showing its folial divisions. fp is exposed by retracting parts of the neighboring f4 and fv. Red spots, positions of the last microelectrode tracks in 21 experiments. Vertical lines 1–5 are drawn at 400, 800, 1,200, 1,600, and 2,000 μm from the caudal pole of fp. (*C*) Coronal section of the left flocculus at the level 4 in *B*. LN, lateral nucleus.

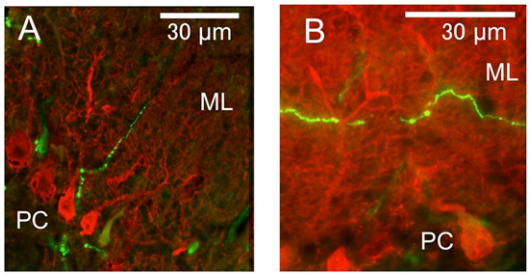

Fig. 2. Orexinergic axons in flocculus. (*A* and *B*) Beaded orexin-immunopositive fibers double-stained for calbindin (red) and orexins (green). ML, molecular layer; PC, Purkinje cell.

Abnormally low basal BP was reported to prevail in genetically orexin-deficient mice (19), but abnormally low basal BP was not the case in our two rabbits systemically injected with orexin receptor-1 (OX-1R) antagonists; mean BP were 92 and 105 mmHg against the control values 98 and 108 mmHg, respectively. In three SAP-treated rabbits, the average of the mean BP was also normal: 92 ± 5 mmHg against 91 ± 3 mmHg in 20 control rabbits. Different neural mechanisms appear to underlie the maintenance of basal BP and the transient BP increase in defense reactions, at least in rabbits.

Involvement of Orexins in Defense Reactions. Under general anesthesia, the hypothalamus was explored with a bipolar needle electrode for stimulation (SE1; Fig. 1). At certain depths along a dorsoventral track, a train of 100-Hz bursts (8-50 pulses; each pulse, 100–500 μA; 0.3 ms wide) effectively induced a transient increase in BP by 20–100 mmHg (Fig. 3*A*, Fig. S2*A*). On the average of mean BP curves (Fig. 3*I*), the mean increase is 49 ± 4 mmHg ($n = 20$) and the mean latency is 0.70 ± 0.03 s ($n = 19$). Four lines of evidence support the view that this transient BP increase is mediated by orexinergic hypothalamic neurons. First, when optimal stimulation sites for this effect were mapped in various experiments (shown in Figs. 3–5 and 7), they covered the region designated as the hypothalamic defense area (Fig. S2*B*) where orexin-immunopositive neurons distributed (Fig. S1*A*). Second, systemic administration (7 mg/kg) of an OX-1R antagonist, SB-334867 (25) or SB-408124 (26), markedly attenuated these BP increases (Fig. 3 *C*, *G*, and *J*). Third, in all of the four rabbits tested 2–6 wk after SAP injection, orexin-immunopositive neurons had largely disappeared from the hypothalamus (Fig. S1*B*; compare with Fig. S1*A*), and, accordingly, hypothalamus stimulation (even as strong as 500 μA) failed to increase mean BP (5 ± 3 mmHg). Note that, in these experiments, the location of the stimulating electrode was controlled stereotaxically to be close to the fornix and later confirmed histologically (for example, * in Fig. S1*B*). Fourth, prepro-orexin–null knockout mice (19) and orexinergic neuron-ablated transgenic mice (20) have been reported to exhibit an attenuated BP increase during hypothalamus stimulation.

Stimulation within or at its border of PAG also induced BP increase as mapped in Fig. S2*D*. As would be expected, this effect was blocked by OX-1R antagonists (Fig. 3 *E* and *G*). We also noted that hypothalamus/PAG stimulation evoked an increase in the rate of integrated electromyograph discharges in nuchal muscles with a latency of ~0.1 s (Fig. 3 *B* and *F*). Importantly, OX-1R antagonists did not affect these motor responses (Figs. 3 *D* and *H*), which suggests that orexins are not involved in motor components of defense reactions (see *Discussion*).

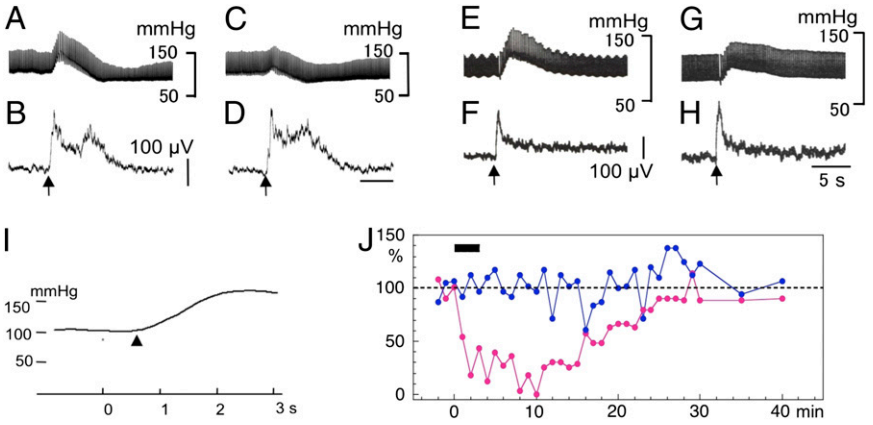

Fig. 3. Defense reactions evoked from the hypothalamus. (*A–D*) Stimulation of hypothalamus. Upward arrows indicate the moments of application of a train of 100-Hz pulses lasting 0.5 s. (*A*) Chart record of BP. (*B*) Integrated EMG recorded from nuchal muscles. (*C and D*) Similar to *A and B*, but recorded 10 min after i.v. injection of SB-334867. (*E–H*) Similar to *A* and *D*, but with stimulation of PAG. (*I*) Twenty times-averaged mean BP curve. ▲, the start of increase. (*J*) Plots changes in peak amplitudes of hypothalamus stimulation-evoked BP increases (red) and short-latency discharges in nuchal muscles (green) after i.v. injection of an OX-1R antagonist.

Orexinergic Excitation of Purkinje Cells. When a glass microelectrode was inserted through the dorsal paraflocculus, it reached ipsilateral fp, neighboring f4, or the ventralmost folium of the ventral paraflocculus (fv), at depths of ∼7 mm (Fig. 1*C*). Sampled Purkinje cells spontaneously discharged simple spikes (Fig. 4 *A* and *B*) at 10–90 spikes per s (mean 40.3 ± 4.0 spikes per s, $n = 28$) and complex spikes at 1–7 spikes per s (mean 3.8 ± 0.3 spikes per s, $n = 19$). Hypothalamus/PAG stimulation on either the left or right side frequently induced a transient increase in the rate of simple spike discharges, as shown in Fig. 4*A*. In peristimulus time histograms (PSTHs), this excitation starts upon stimulation and lasts for a fraction of 1 s to 3–5 s (Fig. 4*C*). The responses occurring within 1 s, with statistical significance in the permutation test (shaded in Fig. 4 *C–E*), were taken as the primary effects of hypothalamus/PAG stimulation.

Among the Purkinje cells sampled in fp and its neighboring folia (fv, f4), 38–40% were excited by hypothalamus stimulation and 27–32% were excited by PAG stimulation (Table S2). When plotted on standardized coronal sections, the vast majority of these excited Purkinje cells were located in fp (Fig. 5 *A* and *C*). The remaining small fraction of excited Purkinje cells protruded into the neighboring f4 (Fig. 5 *A*, *2*; *A*, *3*; *C*, *2*; and *C*, *3*). The hypothalamic origin of the hypothalamus/PAG stimulation-evoked excitation was reflected in the effects of SAP-induced lesions of the hypothalamus; in the lesioned rabbits, hypothalamus stimulation excited Purkinje cells at a significantly lower rate (5%) than in control (38%) or sham-operated (32%) rabbits [Wilcoxon–Mann–Whitney (WMW) test, $P < 0.01$] (Table S2).

When applied iontophoretically at 50 nA through a seven-barreled pipette to individual Purkinje cells (*SI Materials and Methods, Microiontophoresis*), OX-1R antagonists effectively depressed the hypothalamus/PAG stimulation-evoked excitation (Fig. 4*F*). Between before and during iontophoresis, the difference in the histograms was significant in 12 of the 16 cells examined [Wilcoxon signed-rank test for matched samples (WSM) during a 3-s poststimulation period, $P = 0.0001–0.020$]. In this measurement, data obtained using either SB-334867 ($n = 11$) or SB408124 ($n = 5$) and by either hypothalamus ($n = 9$) or PAG stimulation ($n = 7$) were pooled together because these factors made no significant difference in the data obtained. In the absence of hypothalamic/PAG stimulation, iontophoresis of an OX-1R antagonist at 50 nA caused a gradual decrease in the rate of spontaneous simple spike discharges by 40.2 ± 11.6% ($n = 5$; $P = 0.0009$ to <0.0001) on average at 20–29 s (Fig. 4*G*, blue). In contrast, iontophoresis of orexin A at 50 nA rapidly increased the rate of simple spike discharges from Purkinje cells (Fig. 4*G*, red). The average increase observed at 20–29 s after the onset of iontophoresis was 40.4 ± 6.6% [$n = 5$; Wilcoxon test for single samples (WSS) $P = 0.02–0.006$]. These observations indicate that in fp Purkinje cells, orexins are spontaneously released to provide a background excitation and also mediate the hypothalamus/PAG stimulation-evoked excitation. Because the ionotophoresis of 6-cyano-7-nitroquinoxaline-2, 3-dione (CNQX), an alpha-amino-3-hydroxy- 5-methyl-4-isoxazole propionate (AMPA) receptor antagonist did not affect hypothalamus/PAG-stimulation-induced excitation (Fig. S3, $n = 4$), it is unlikely that Purkinje cells were excited by glutamate that might be coreleased with orexins.

Nonorexinergic Inhibition of Purkinje Cells. The hypothalamus/PAG stimulation at sites optimal for induction of the rapid BP rise

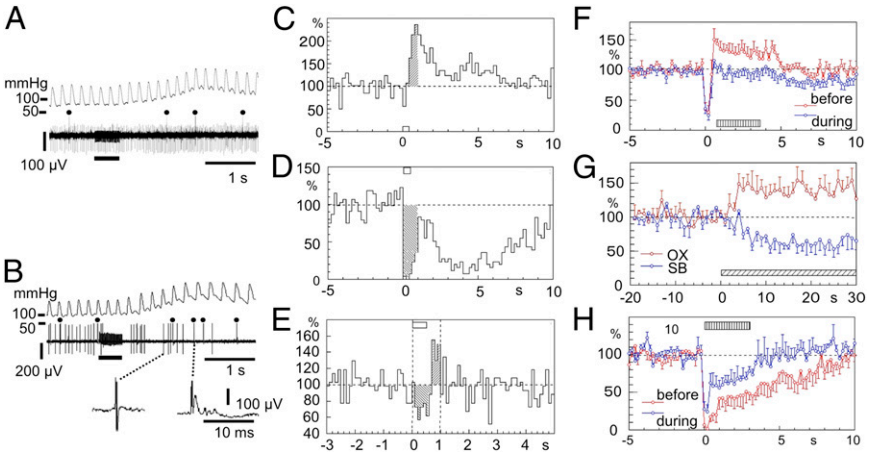

Fig. 4. Recording from Purkinje cells. (*A*) Upper record, BP. Lower record, simple and complex spike discharges. Dots indicate complex spikes. The left hypothalamus was stimulated (horizontal bar). (*B*) Similar to *A*, but for another Purkinje cell. Specimens of simple and complex spikes are shown in an expanded time scale. (*C–E*) Examples of PSTHs for simple spike responses to hypothalamus/PAG stimulation. Ordinates, simple spike discharge frequency relative to the average frequency during 5-s prestimulation periods. Deviations of the PSTHs from that level occurring during 1-s poststimulation periods are shaded. Squares indicate the period of the stimulation. (*F*) Averaged PSTHs showing excitation before (red) and during (blue) continuous application of OX-1R antagonists at 100 nA ($n = 16$). A vertically hatched band indicates the 3-s period for statistical comparison between the two groups of plots. (*G*) Effects of iontophoresis of orexin-A (red) or OX-1R antagonists (blue) on spontaneous simple spike discharges. An obliquely hatched band indicates iontophoresis ($n = 5$ for each of the red and blue plots). (*H*) Similar to *F*, but with the effect of continuous iontophoresis of bicuculline on hypothalamus/PAG-induced inhibition ($n = 5$).

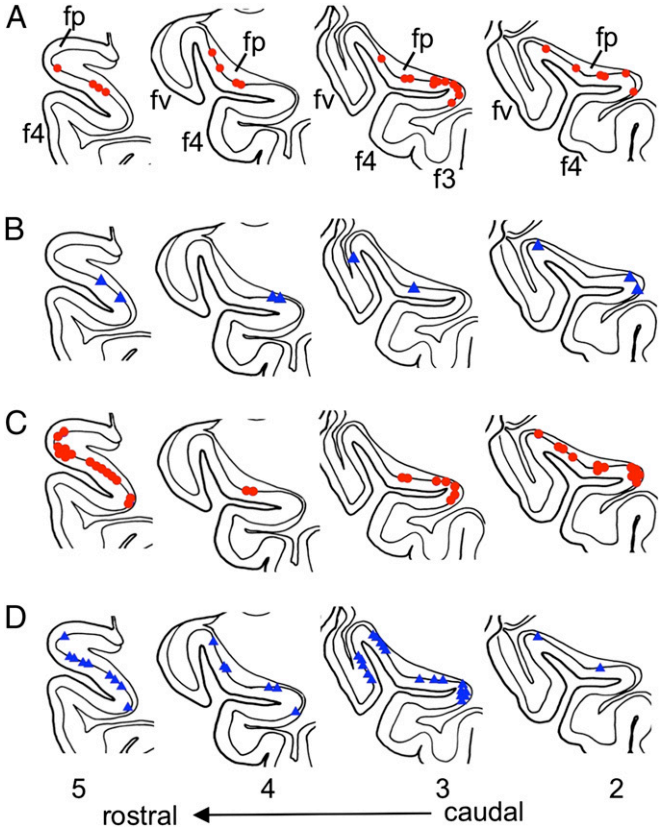

Fig. 5. Location of hypothalamus/PAG stimulation-excited or -inhibited Purkinje cells. The 2–5, coronal sections of a standard flocculus specimen drawn at four levels indicated in Fig. 1*B*. The sites recording from Purkinje cells were determined on serial coronal sections and then replotted on the most closely positioned specimen section. (*A*) Hypothalamus stimulation-excited Purkinje cells (in red). (*B*) Hypothalamus stimulation-inhibited Purkinje cells (in blue). (*C* and *D*) Similar to *A* and *B*, but with PAG stimulation. Data were obtained from 7 rabbits with hypothalamus stimulation and 13 rabbits with PAG stimulation.

(Fig. S2) induced not only excitation in a population of Purkinje cells in and near fp (see above) but also inhibition in another overlapping population of them (Fig. 4 *B* and *D*). The inhibited and excited Purkinje cells were mixed side by side (Fig. 5 *B* and *D*), and, in some Purkinje cells, excitation and inhibition appeared in succession (Fig. 4*E*), indicating that both excitation and inhibition converged to these Purkinje cells.

However, the inhibition should have nonhypothalamic origins because SAP lesions in the hypothalamus did not impair the inhibition (Table S2); for example, left hypothalamus stimulation in SAP-treated rabbits inhibited 56% of the Purkinje cells examined compared with 46% in control or 51% in sham-operated rabbits. Note also that iontophoresis of OX-1R antagonists did not affect the inhibition (Fig. 4*F*; see the inhibition phase at 0–1 s). Therefore, it is likely that the inhibition arises from nonorexinergic neurons, which might be located outside of the hypothalamus but extending their axons through the hypothalamus. Because bicuculline applied at 10–20 nA effectively attenuated the inhibition on average by 37 ± 4% ($n = 5$; WSM, $P = 0.01576$–0.00042) (Fig. 4*H*), the inhibition should be mediated by GABA, at least in part.

Note that PAG stimulation evoked inhibition at a considerably higher rate (68–74%) than hypothalamus stimulation (45–46%) (Table S2). Note also that Purkinje cells inhibited by PAG stimulation extended laterally into fv (Fig. 5 *D*, *3*). It may be that the inhibition evoked from hypothalamus and that evoked from PAG are mediated by a different pathway(s), at least in part. A question may arise how the nonorexinergic inhibition in fp Purkinje cells contributes to defense reactions. However, we leave this question open until we determine origins of the inhibition.

Input–Output Connections of fp. For axonal tracing, we first used DiI for its special advantage that it could be applied precisely to fp in formol-fixed postmortem cerebella under direct vision (27). In seven such brain specimens, we observed DiI-labeled axons of fp Purkinje cells to form a bundle that seemingly extended to the ipsilateral PBN, displaying an axon terminal-like varicose pattern there (Fig. 6 *A* and *B*). These fibers could be axons of fp Purkinje cells projecting to PBN, but the possibility cannot be excluded that these are in part retrogradely labeled afferent fibers to fp. In fact, some PBN neurons were retrogradely labeled (see Fig. 6*C* and below). We then adopted anterogradely transported biotinylated dextran amine (BDA) (28) and injected stereotaxically to the fp. In the case of such injection shown in Fig. 6 *D*–*F*, we observed axon terminal-like structures (*F*) in the ventrolateral corner of the ipsilateral PBN (*E*). The injected BDA extended to f1–f4 folia (*D*); however, because no evidence was obtained in previous studies that Purkinje cells in these non-fp folia project to PBN, it would be reasonable to assume that the BDA-labeled axon terminal-like structures in PBN originated from fp Purkinje cells (*Discussion*).

Those neurons retrogradely labeled by DiI from fp (Fig. 6*C*) are a possible source of mossy fibers projecting to fp. We counted 177 retrogradely labeled neurons in the PBN of seven rabbits, among which 126 lay in the lateralmost part of the PBN and the remaining 51 in the medial subnucleus. In one rabbit, WGA-HRP injected into fp also retrogradely labeled neurons in the pedunculopontine nucleus (PPN) (Fig. S4 *E* and *F*). A few dispersed hypothalamus neurons were also labeled (Fig. S4 *C* and *D*) in the manner reported previously by Haines et al. (1984) (29). They could be orexinergic neurons. DiI injected into fp also labeled retrogradely neurons in the contralateral inferior olivary nucleus (ION). In four rabbits, 113 DiI-labeled neurons were located in the caudolateral portion of the principal olive (Fig. 6 *G* and *H*). WGA-HRP (*SI Materials and Methods*, *HRP Labeling*) injected into fp also labeled neurons in this ION area (Fig. S4*B*). These ION neurons are presumed to be the origin of climbing fibers projecting to fp.

Climbing Fiber Signals. We explored the peripheral sources of climbing fiber signals to fp Purkinje cells and found that a significant (permutation test, $P = 0.00033$–0.048) transient increase in the rate of climbing fiber discharges occurred under the following three conditions: (*i*) electric pulse stimulation of the aortic nerve; a significant effect occurred in four of the six Purkinje cells examined, with latencies of 0.06–0.14 s (Fig. 7*A*); (*ii*) electric hypothalamic stimulation that caused a rapid BP increase; a significant effect occurred in 10 of the 21 Purkinje cells examined, with latencies of 0.5–2.0 s (Fig. 7*B*); and (*iii*) quick one-shot injections of 40 mM KCl solution (4 mL at a time) to hindlimb muscles via left iliac artery; a significant effect occurred within a few seconds after the onset of the injection in 10 of the 20 Purkinje cells tested (Fig. 7*C*). Implications of these three types of stimulus are later discussed (*Discussion*). When hypothalamus/PAG stimulation-excited Purkinje cells were selected, significant increases in the climbing fiber discharge rate were observed in 2/2, 8/11, and 6/11 cells tested under the above-mentioned three conditions. The overall frequency of occurrence was 16 of the 24 excited Purkinje cells (67%). That similarly calculated for hypothalamus/PAG stimulation-inhibited Purkinje cells was 8/23 (35%), half of that for excited cells.

Arterial Blood Flow and BP in Behaving Rabbits. Electric foot shock stimuli (FS) evoke defense reactions in a freely moving animal (30). We adopted 2–4 mA stimuli, lasting 1, 3, or 30 s, as FS. These stimuli evoked quick turning-around locomotion of the rabbit within the cage. Trials were repeated once every 10 min four to seven times in one session to obtain averaged responses

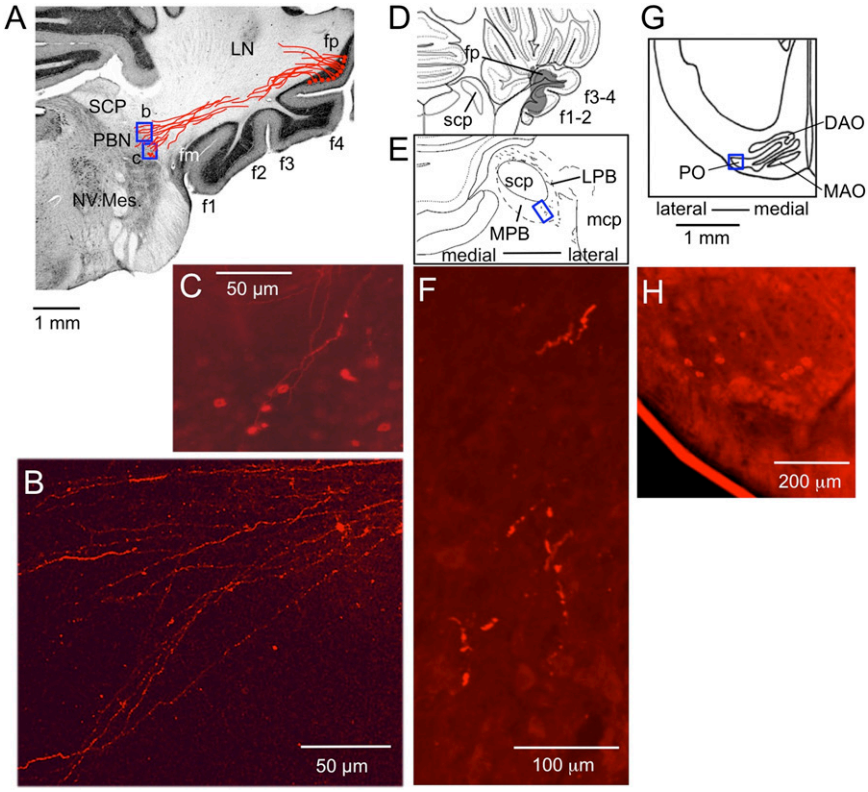

Fig. 6. DiI- and BDA-labeled outputs and inputs of fp. (*A*) Coronal sections of cerebellum and medulla through right fp, into which DiI was injected. DiI-containing fibers were traced through three consecutive sections (100 μm thick) and superposed as drawn in red. LN, lateral cerebellar nucleus; NV. Mes., mesencephalic trigeminal nucleus; SCP, superior cerebellar peduncle. (*B* and *C*) Photomicrographs for two small areas (b and c) enclosed in *A* showing varicous pattern of the labeled axons (*B*) and retrogradely labeled neurons (*C*), respectively. (*D*) A section of the brainstem of another rabbit, relatively rostral corresponding to the level 5 in Fig. 4. BDA covered fp but extended also to the other floccular folia. (*E*) A 45-μm-thick section cut at 810 μm caudal to *D*, showing tissues around SCP in a larger scale. Wavy short lines indicate BDA-labeled axons. LPB, lateral PBN; MPB, medial PBN; mcp, middle cerebellar peduncle. (*F*) A photomicrograph of the part enclosed by a rectangle in *E* showing axon terminal-like structure labeled by BDA. (*G*) A section of the ventrolateral medulla at the caudal level of the principal olive (PO) of a third rabbit. Only the side contralateral to the fp injected with DiI is shown. (*H*) A photomicrograph for the area enclosed by a square in (*G*) showing retrogradely labeled IO neurons.

to FS. In each rabbit, a session was repeated several times at intervals of 6–7 d.

In the first set of experiments, probes for arterial blood flow were attached to the right and/or left femoral artery that supplies leg muscles, or one to the celiac artery that supplies major visceral organs. In rabbits in the control state (Fig. 8*A*, curves a and b), each FS regularly induced transient increases in the femoral arterial flow (FAF) and simultaneous decreases in the visceral arterial flow (VAF), representing the redistribution of arterial blood flow from visceral organs to active muscles. We measured the average increase of FAF or decrease of VAF during the 30 s of FS stimulation relative to their prestimulation magnitude; FS increased FAF by 75 ± 12% ($n = 7$; n in this section means the number of rabbits used) and decreased VAF by 53 ± 7% ($n = 8$). Fig. 8*A* also shows that i.v. one-shot injection of an OX-1R antagonist (7 mg/kg) decreased FS-induced changes in both FAF and VAF (curves c and d). These decreases were relatively short-lasting and diminished in 20 min. As compared just before and within 15 min after the injection, the FS-induced FAF increases were depressed by 57 ± 9% ($n = 5$; t test, $P = 0.008$), and the FS-induced VAF decreases were depressed by 54 ± 12% ($n = 4$; $P = 0.034$).

After these measurements, kainate solution (0.1%, 1 μL at a time) was injected to fps bilaterally under general anesthesia. When measured more than 5 d later, the amount of 30-s FS-induced FAF enhancement was 2.33 ± 0.29 ($n = 3$) times larger than that before the kainate treatment (t test, $P = 0.037$). In contrast, the amount of FS-induced VAF reduction was smaller, 0.39 ± 0.12 ($n = 3$) times that before the kainate treatment (t test, $P = 0.045$). It was also noted (Fig. 8*B*, curves e and f) that the time course of 30-s FS-evoked VAF decrease became significantly faster; half-decay time was reduced from 20 to 24 s to 6 to 15 s (by 45 ± 9%, $n = 3$; t test $P = 0.028$) after the kainate treatment. The half decay time for FAF increase also became shorter from 60 to 100 s to 24 to 58 s, by 59 ± 15% ($n = 3$) on average, but this shortening is not statistically significant ($P = 0.108$).

In the second set of experiments, mean BP was measured at the right femoral artery. In the control state, 30-s FS regularly caused a modest increase of mean BP (20 ± 3 mmHg, $n = 7$). During 30-s FS, the increased BP began to decrease and, after the cessation of FS, further decreased to the prestimulation level or slightly below that (Fig. 8*C*, curve g). FS for 1 or 3 s induced changes in mean BP somewhat smaller in amplitude but similar in time course to those induced by 30-s FS (see below). These rabbits then received bilateral kainite treatment, and FS-induced changes in the mean BP were measured 6 d thereafter. In one rabbit, 30-s FS caused a 16-mmHg decrease instead of the 16-mmHg increase observed before the kainite treatment (Fig. 8*C*, curve h). In another rabbit, 30-s FS caused a 10-mmHg increase of the mean BP, but this increase was smaller than the 25-mmHg increase observed before kainate treatment. A third rabbit was tested with 1-s FS, which caused a 15-mmHg increase in the mean BP before but a 10-mmHg decrease after kainate treatment. These observations consistently suggest that the fp normally acts to maintain BP at a modestly enhanced level during defense reactions.

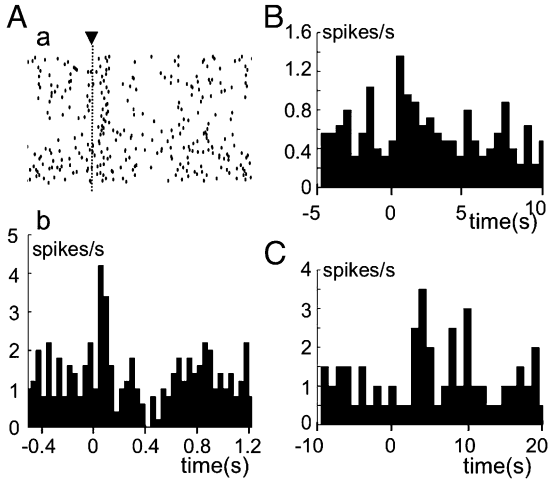

Fig. 7. Sources of climbing fiber signals. Complex spikes were recorded from fp Purkinje cells and distinguished from simple spikes by their characteristic configurations. (*A*) Raster diagram (*a*) and corresponding PSTH (*b*) for complex spike discharges evoked from an fp Purkinje cell. ▼, moment of stimulation of the right aortic nerve with electric single pulses. Ordinate in *b*, discharge rate of complex spikes/s. (*B*) PSTH of complex spikes evoked by hypothalamic stimulation (time at 0 s) that induced transient mean BP increase. (*C*) Similar to *B*, but for one-shot injection of 40 mM KCl solution into left iliac artery at time 0 s.

Discussion

Neuronal Circuit for Cardiovascular Defense Reactions. On the basis of previous reports from many authors and the present data, Fig. 9 delineates the neuronal circuit for cardiovascular defense reactions. As the cardiovascular defense reactions are typically evoked by an electric foot shock (Fig. 8), they should primarily involve a somatosympathetic reflex (SSR) (31), which is evoked by stimulation of the skin, joints, or muscles; after these reactions are mediated by a segmental circuit (SGC), they act upon the sympathetic preganglionic neurons located in the intermediolateral nucleus (IML) of the spinal cord. The activated IML may then generate spatiotemporal patterns of arterial blood flow among muscles and visceral organs (23, 32). A supraspinal pathway (SSP) involving spinal and trigeminal sensory nuclei (SVN) (33) and sympathetic premotor neurons in the rostroventrolateral nucleus (RVL) superposes on the SSR pathway. Another pathway mediated by PBN neurons further parallels SSP; PBN neurons receive excitatory inputs from various sensory pathways including PPN (34) and in turn project to RVL (35). According to a general finding in vestibular/cerebellar nuclei (2), we assume that various inputs to PBN are derived from collaterals of mossy fibers (Fig. 9). RVL forms a complex neuronal circuit with other cardiovascular brainstem nuclei (for review, see ref. 36), including the nucleus tractus solitarius (NTS). NTS receives baroreceptor signals and in turn activates the caudal ventrolateral medulla (CVL), which inhibits RVL, forming the baroreflex pathway. Eventually, NTS also projects to vagal cardioinhibitory (VCI) neurons, adding to the baroreceptor reflex (BRR). The paraventricular nucleus of the hypothalamus may also contribute to cardiovascular defense reactions via two-way connections with NTS, but these connections are left out from Fig. 9 for simplicity.

In this study, DiI injected into fp under direct vision labeled a bundle of axons that course between fp and the ventrolateral corner of PBN (Fig. 6 *A* and *B*). This bundle, at least in part, would contain axons of fp Purkinje cells directly projecting to PBN. BDA stereotaxically injected into fp labeled axon terminal-like structures in the ventrolateral corner of PBN (Fig. 6 *D–F*), supporting the view that fp Purkinje cells project directly to the ventrolateral corner of PBN. Even though the injected BDA spread to f1–f4 (Fig. 6*D*), previous studies revealed no Purkinje cell projection from these non-fp folia to PBN (9, 37, 38). Therefore, it is likely that the cells projecting to PBN were fp Purkinje cells, presumably for control of cardiovascular defense reactions. Note that a previous study also revealed a direct projection of fp Purkinje cells to vestibular nuclei [see figures 2 and 3 of Tan et al. (9)]. Therefore, fp Purkinje cells could also be involved in some vestibular function. This finding is in agreement with that reported for the lateral nodulus–uvula area, from which Purkinje cells project to not only PBN but also vestibular nuclei (7). Lesioning of this area impaired cardiovascular adjustment to changes in head position and posture, suggesting that Purkinje cells in this area contribute to the control of vestibulosympathetic reflexes (39). One may suppose that fp is involved in not only SSRs but also a certain vestibulo-autonomic function during defense reactions; this function, however, has yet to be specified.

How is the circuit in Fig. 9 coupled with motor activities such as quick locomotion in defense behavior? One way is feedback from active muscles via mechanoreceptors or K^+ release. However, in this study, we recognized that a hypothalamus/PAG stimulation evoked short latency activity in nuchal muscles (Fig. 3 *B* and *F*), which suggests the presence of a feedforward central command that drives motor systems (40). This central command was not affected by systemic administration of OX-1R antagonists (Fig. 3 *D* and *H*). We may suppose that a nonorexinergic central command comes from the mesencephalic locomotor region, but presently we have little knowledge about its origin or relation to the feedback from active muscles via mechanoreceptors or K^+ release.

Orexinergic Neuromodulation. We have shown that orexin-immunopositive fibers originate from the classic defense area in the hypothalamus, extend branches through PAG, and reach the flocculus with the highest density in fp. Two lines of evidence indicate that these fibers mediate the hypothalamus/PAG stimulation-induced excitation of fp Purkinje cells. First, OX-1R antagonists effectively depressed this excitation (Fig. 4*F*). Second, SAP-induced lesions of hypothalamic neurons markedly decreased the frequency of occurrence of the excitation among fp

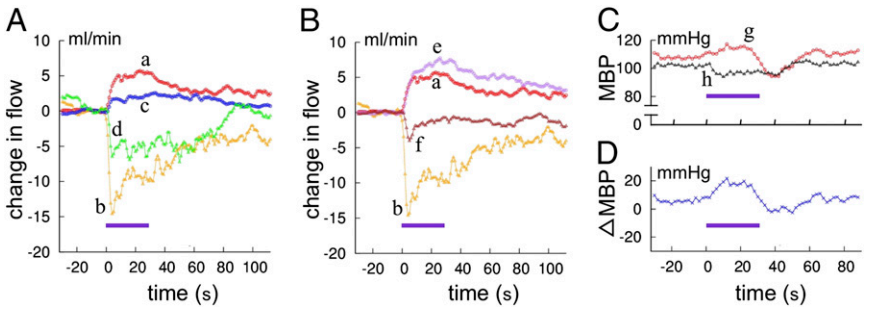

Fig. 8. Electric foot shock-evoked changes of arterial blood flow and blood pressure. (*A*) Redistribution of arterial blood flow. Curves a and b indicate control FAF and VAF, and the superposed curves c and d indicate FAF and VAF following systemic administration of OX-1R antagonist. Each curve indicates an average of four trials in the same session. (*B*) Changes in arterial blood flow recorded in the same rabbit as that whose data are shown in *A* before (curves a and b, same data as in *A*) and 5 d after kainite injection into bilateral fp regions (curves e and f, average of six trials). (*C*) Changes in mean BP (MBP) evoked by foot-shock stimulation. Curve g, before kainite lesioning; curve h, after kainate lesioning. (*D*) Difference between the curves g and h. Horizontal bars indicate the period of foot shock stimulation.

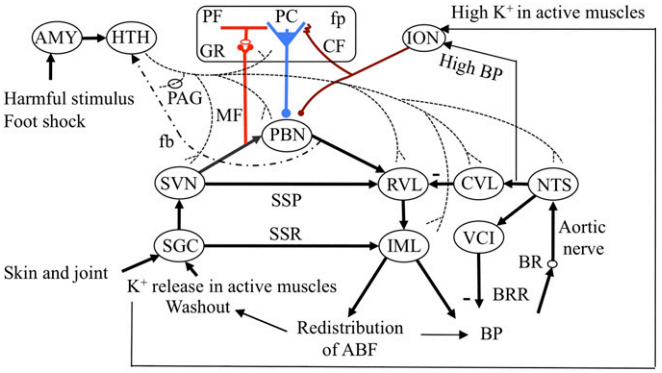

Fig. 9. Neuronal circuit diagram for cerebellar control of defense reactions. AMY, amygdala; BR, baroreceptor; CF, climbing fiber; fb, feedback pathway; GR, granule cell; HTH, hypothalamus; MF, mossy fber; PF, parallel fiber. Other abbreviations are defined in the text.

Purkinje cells (Table S2). Therefore, despite their dispersed diffuse distribution in fp (Fig. 2), the orexin-immunopositive fibers prove to exert a substantial excitatory action on Purkinje cells. Peculiarly, there has been no literature confirming a significant presence of OX-1 or OX-2 mRNA in the cerebellum of rodents (41). Nevertheless, the absence of mRNA in cell somata may not exclude the possibility that proteins of OX-1 or OX-2 exist in peripheral dendrites.

Orexin-immunopositive fibers are sparsely distributed and form diffuse connections to their target neurons not only in fp but also in broad areas of the brainstem, including PBN (42). This fact implies that orexins released from these fibers do not provide input/output-specific information, but they govern the general activity of their target neurons and thereby switch the operational mode of the target neuronal circuit in the manner of neuromodulation (43). In Fig. 9, the dashed line labeled fb represents a return projection from the PBN to the hypothalamic region where orexinergic neurons distribute (44). This projection may feed back orexin-evoked activities in the medulla and cerebellum to hypothalamic orexinergic neurons. Orexins act on G protein-coupled receptors (45) and excite target neurons (46) by inducing membrane depolarization via a decrease in membrane conductance for potassium ions (47), and possibly also via Ca^{2+} entry through transient receptor potential cation (TRPC) channels (48).

Innately fearful or fear-conditioned stimuli activate hypothalamic orexinergic neurons via the amygdala (18). Activated orexinergic neurons would switch the cardiovascular defense system to an alert mode from other modes. Peripheral stimuli would then sensitively evoke defense reactions. In a nonalert mode, in which orexinergic neurons are inactive, the same peripheral stimuli may not evoke defense reactions. This conjecture is supported by the present finding that systemic administration of OX-1R antagonists depressed the FS-evoked defense reactions (Fig. 8*A*). The present study provides a prototype of the selection mechanism for behavioral repertoires via neuropeptidergic or aminergic neuromodulation. Each peptide or amine may associate with a set of structures through the spinal cord, brainstem, and cerebellum, which jointly express a specific behavior.

Orexinergic fibers impinge also fm and f1–f4, less densely than in fp but still significantly (Table S1). From these floccular folia, Purkinje cells project axons to vestibular nuclear neurons mediating the vestibuloocular reflex (37, 38), but roles of orexins in this reflex has not been clarified. Orexin A excites lateral vestibular nuclear neurons and improves vestibular-related motor behavior in rats (49), but the relevance of these neurons to the flocculus remains unclear.

Cerebellar Control of Cardiovascular Defense Reactions. We found that Purkinje cells in fp receive climbing fiber signals via the aortic nerve (Fig. 7*A*), which arise from baroreceptors that sense an increase in BP. Climbing fiber signals were also induced by the hypothalamic stimulation (Fig. 7*B*). Because the latencies of these signals (0.5–2.0 s) match those of the hypothalamus stimulation-evoked BP increase (0.5–1.0 s, see Fig. 3*I*), it is likely that climbing fiber signals are evoked as a consequence of the transient BP increase. During the FS-induced redistribution of arterial blood flow, BP increased modestly (by 20 mmHg; see *Results*), and therefore the hypothalamus/PAG stimulation-evoked relatively large BP increase (by 49 mmHg, see *Results*) should imply errors in cardiovascular control. Intraarterial injection of a high-potassium solution into muscles (Fig. 7*B*) should also represent errors because it mimics the failure of sufficient removal of potassium secreted from contracting muscle fibers by an increased arterial blood flow. Potassium accumulated in the interstitial space of active muscles stimulates group III and IV afferents (50, 51). Activities of these afferents will eventually reach the inferior olive as error signals. To summarize, fp appears to adaptively control arterial blood flow to avoid an excessive rise of BP and accumulation of potassium in active muscles during defense reactions. This interpretation is consistent with the general view that a cerebellar circuit learns by referring to climbing fiber error signals (2).

In Fig. 9, fp is connected to the neuronal circuits for cardiovascular defense reactions (SSP and SSR; see above) via PBN. Comparison of FS-induced responses before and after fp lesioning (Fig. 8 *B*, *C*, and *D*) revealed twofold roles of fp in defense reactions. First, after fp lesioning, FS-induced FAF increases became significantly larger whereas FS-induced VAF decreases became significantly smaller and shorter-lasting. Apparently, fp normally functions for effectively balancing arterial blood flow in magnitude and time course between active muscles and visceral organs/resting muscles. This balancing function must be mediated by the sympathetic nervous system that regulates vasodilatation and vasoconstriction. Second, fp lesioning impaired FS-induced modest BP increases, which either decreased or were converted to decreases (Fig. 8*D*). Because BP is a function of vascular resistance and cardiac output, fp may regulate BP in defense reactions by adjusting vaso-dilatation/-constriction among arteries to achieve appropriate total vascular resistance. The role of fp in defense reactions can thus be interpreted consistently with the cerebellar adaptive control system model (2).

Materials and Methods

Animals. Male adult albino rabbits (2.4–3.1 kg) were obtained from Japan SLC Inc. and were housed in an environment-controlled, 12-h-light/12-h-dark room, receiving water and food ad libitum. In addition, male young (1.0 kg) albino rabbits were similarly obtained, and they were used only for DiI tracing. We followed the Guidelines for the Care and Use of Laboratory Animals of RIKEN. The Wako Animal Experiment Committee of RIKEN approved the plan of our experiments.

Standard Surgery. A rabbit was anesthetized by an i.v. injection of urethane (600 mg/kg body weight) and α-chloralose (60 mg/kg body weight), artificially respired, and mounted on a stereotaxic frame in a prone position. In acute experiments, BP was monitored through a heparin-filled polyethylene tube inserted into the abdominal aorta through the right femoral artery and connected to a pressure gauge (MP-3, AP-600G, Nihon Kohden). After each experiment, the rabbit was deeply anesthetized and perfused transcardially with 1 L of PBS mixed with 10,000 units of heparin and then with 1.5 L of ice-cold 4% paraformaldehyde in PBS.

Lesioning. Under urethane-α-chloralose–induced anesthesia, 490 ng of SAP (Advanced Targeting Systems) in 0.5 μL of PBS (Otsuka) or 980 ng of SAP in 2 μL of PBS was injected at one time to the hypothalamus using a Hamilton syringe, bilaterally or unilaterally. In sham-operated rabbits, 1 μL of PBS solution was bilaterally injected to the hypothalamus. Kainate solution (0.1%, 1 μL at a time) was injected stereotaxically into bilateral fp regions. Later histological examinations revealed the loss of Purkinje cells over large parts of fp (Fig. S5).

Recording from Purkinje Cells. Glass microelectrodes were filled with a solution containing 2 M NaCl and Fast Green FCF dye (electric resistance, 3–5

Mohm). Unit spikes of Purkinje cells conventionally recorded were analyzed with a MAP System (Plexon Inc.) using MAP control software (RASPUTIN). To analyze PSTHs, we adopted nonparametric statistical methods (WMW, WSS, WSM). The permutation test of two independent data sets was also used (*SI Materials and Methods, Statistical Analysis*).

Iontophoretic Drug Application. Drugs were applied to Purkinje cells iontophoretically through seven-barreled micropipettes (*SI Materials and Methods, Microiontophoresis*). Each barrel was filled with one of the following solutions: 20 mM bicuculline methochloride in 0.165 M NaCl (pH 4.0), 4 mM CNQX in 0.154 M NaCl (pH 7.0), 0.3 mM orexin-A (pH 7.0), or 0.5 mM SB334867/SB408124 in 0.165 M NaCl (0.1% DMSO) (pH 6.0). All of the drugs were purchased from Tocris or Sigma.

Axonal Transport Tracers. Tetramethylrhodamine and biotin conjugated Dextran (10,000 MW, Lysin fixable, D-3312) and a vector (VECTASTAIN ABC Kit, Standard, PK-4000) were purchased from Molecular Probes. The 0.02–0.1 μL of 5% solution at a time was injected to fp bilaterally (28). One week later, the brain tissues were cut to thin sections (45 μm thick).

1,1-Dioctadecyl-3,3,3′,3′-tetramethyl-indocarbocyanine perchloride (DiI) was purchased from Invitrogen Molecular Probes TH. Under direct vision of a formalin-fixed cerebellum, a DiI crystal was placed on fp and pushed into the cortex using a needle, or 50% ethanol solution with dissolved DiI was injected into fp (27). More than 4 mo later, the brain tissues were cut into serial sections (100 μm).

Behavioral Tests. To monitor arterial blood flow, an ultrasonic pulse Doppler flow meter (VF-1, PD-20/10, Christal Biotech) was used. To monitor BP by radiotelemetry (Primetech; TA11PA-D-70), a probe was chronically embedded in the abdominal cavity and connected to the abdominal aorta. Defense reactions were tested in a cage (size 48 × 48 × 45 (height) cm). The top of the box was open. The floor was a grid that was connected to a shock generator (scrambler, SGS-003DX; Muromachi).

Details of the methods used, figures of a confirmatory nature, and numerical data are shown in *SI Materials and Methods*.

ACKNOWLEDGMENTS. We thank Mr. Masahiro Ito, Ms. Mari Ito-Shiga, Dr. Mari Anzai, and Ms. Moeko Kudo for technical assistance. We are grateful for the continuous support given by RIKEN Brain Science Institute.

1. Oscarsson O (1979) Functional units of the cerebellum-sagittal zones and microzones. *Trends Neurosci* 2:144–145.
2. Ito M (2006) Cerebellar circuitry as a neuronal machine. *Prog Neurobiol* 78(3-5): 272–303.
3. King JS, Cummings SL, Bishop GA (1992) Peptides in cerebellar circuits. *Prog Neurobiol* 39(4):423–442.
4. Ito M (2009) Functional roles of neuropeptides in cerebellar circuits. *Neuroscience* 162(3):666–672.
5. Schweighofer N, Doya K, Kuroda S (2004) Cerebellar aminergic neuromodulation: Towards a functional understanding. *Brain Res Brain Res Rev* 44(2-3):103–116.
6. Paton JFR, Spyer KM (1990) Brain stem regions mediating the cardiovascular responses elicited from the posterior cerebellar cortex in the rabbit. *J Physiol* 427:533–552.
7. Sadakane K, Kondo M, Nisimaru N (2000) Direct projection from the cardiovascular control region of the cerebellar cortex, the lateral nodulus-uvula, to the brainstem in rabbits. *Neurosci Res* 36(1):15–26.
8. Nagao S, Ito M, Karachot L (1985) Eye field in the cerebellar flocculus of pigmented rabbits determined with local electrical stimulation. *Neurosci Res* 3(1):39–51.
9. Tan J, Epema AH, Voogd J (1995) Zonal organization of the flocculovestibular nucleus projection in the rabbit: A combined axonal tracing and acetylcholinesterase histochemical study. *J Comp Neurol* 356(1):51–71.
10. Nambu T, et al. (1999) Distribution of orexin neurons in the adult rat brain. *Brain Res* 827(1-2):243–260.
11. de Lecea L, et al. (1998) The hypocretins: Hypothalamus-specific peptides with neuroexcitatory activity. *Proc Natl Acad Sci USA* 95(1):322–327.
12. Sakurai T, et al. (1998) Orexins and orexin receptors: A family of hypothalamic neuropeptides and G protein-coupled receptors that regulate feeding behavior. *Cell* 92(4):573–585.
13. Chemelli RM, et al. (1999) Narcolepsy in orexin knockout mice: Molecular genetics of sleep regulation. *Cell* 98(4):437–451.
14. Nisimaru N, Ito M (2005) *35th International Congress of Physiological Sciences, March 31–April 5, 2005: Abstracts* (Federation of American Societies for Experimental Biology, Bethesda, MD).
15. Silveira MCL, Graeff FG (1992) Defense reaction elicited by microinjection of kainic acid into the medial hypothalamus of the rat: Antagonism by a $GABA_A$ receptor agonist. *Behav Neural Biol* 57(3):226–232.
16. Markgraf CG, et al. (1991) Hypothalamic, midbrain and bulbar areas involved in the defense reaction in rabbits. *Physiol Behav* 49(3):493–500.
17. Adams DB, Baccelli G, Mancia G, Zanchetti A (1969) Cardiovascular changes during naturally elicited fighting behavior in the cat. *Am J Physiol* 216(5):1226–1235.
18. Sakurai T (2007) The neural circuit of orexin (hypocretin): Maintaining sleep and wakefulness. *Nat Rev Neurosci* 8(3):171–181.
19. Kayaba Y, et al. (2003) Attenuated defense response and low basal blood pressure in orexin knockout mice. *Am J Physiol Regul Integr Comp Physiol* 285(3):R581–R593.
20. Zhang W, Sakurai T, Fukuda Y, Kuwaki T (2006) Orexin neuron-mediated skeletal muscle vasodilation and shift of baroreflex during defense response in mice. *Am J Physiol Regul Integr Comp Physiol* 290(6):R1654–R1663.
21. Supple WF, Jr., Kapp BS (1994) Anatomical and physiological relationships between the anterior cerebellar vermis and the pontine parabrachial nucleus in the rabbit. *Brain Res Bull* 33(5):561–574.
22. Chamberlin NL, Saper CB (1992) Topographic organization of cardiovascular responses to electrical and glutamate microstimulation of the parabrachial nucleus in the rat. *J Comp Neurol* 326(2):245–262.
23. Koba S, Xing J, Sinoway LI, Li J (2007) Differential sympathetic outflow elicited by active muscle in rats. *Am J Physiol Heart Circ Physiol* 293(4):H2335–H2343.
24. Gerashchenko D, Chou TC, Blanco-Centurion CA, Saper CB, Shiromani PJ (2004) Effects of lesions of the histaminergic tuberomammillary nucleus on spontaneous sleep in rats. *Sleep* 27(7):1275–1281.
25. Smart D, et al. (2001) SB-334867-A: The first selective orexin-1 receptor antagonist. *Br J Pharmacol* 132(6):1179–1182.
26. Langmead CJ, et al. (2004) Characterisation of the binding of [3H]-SB-674042, a novel nonpeptide antagonist, to the human orexin-1 receptor. *Br J Pharmacol* 141(2):340–346.
27. Honig MG, Hume RI (1989) DiI and diO: Versatile fluorescent dyes for neuronal labelling and pathway tracing. *Trends Neurosci* 12(9):333–335, 340–341.
28. Veenman CL, Reiner A, Honig MG (1992) Biotinylated dextran amine as an anterograde tracer for single- and double-labeling studies. *J Neurosci Methods* 41(3):239–254.
29. Haines DE, Dietrichs E, Sowa TE (1984) Hypothalamo-cerebellar and cerebello-hypothalamic pathways: A review and hypothesis concerning cerebellar circuits which may influence autonomic centers affective behavior. *Brain Behav Evol* 24(4): 198–220.
30. Passerin AM, et al. (2000) Role of locus coeruleus in foot shock-evoked Fos expression in rat brain. *Neuroscience* 101(4):1071–1082.
31. Sato A, Schmidt RF (1973) Somatosympathetic reflexes: Afferent fibers, central pathways, discharge characteristics. *Physiol Rev* 53(4):916–947.
32. Kerman IA, Yates BJ (1999) Patterning of somatosympathetic reflexes. *Am J Physiol* 277(3 Pt 2):R716–R724.
33. Cechetto DF, Standaert DG, Saper CB (1985) Spinal and trigeminal dorsal horn projections to the parabrachial nucleus in the rat. *J Comp Neurol* 240(2):153–160.
34. Plowey ED, Kramer JM, Beatty JA, Waldrop TG (2002) In vivo electrophysiological responses of pedunculopontine neurons to static muscle contraction. *Am J Physiol Regul Integr Comp Physiol* 283(5):R1008–R1019.
35. Miura M, Takayama K (1991) Circulatory and respiratory responses to glutamate stimulation of the lateral parabrachial nucleus of the cat. *J Auton Nerv Syst* 32(2):121–133.
36. Guyenet PG (2006) The sympathetic control of blood pressure. *Nat Rev Neurosci* 7(5): 335–346.
37. Yamamoto M (1978) Localization of rabbit's flocculus Purkinje cells projecting to the cerebellar lateral nucleus and the nucleus prepositus hypoglossi investigated by means of the horseradish peroxidase retrograde axonal transport. *Neurosci Lett* 7(2-3):197–202.
38. De Zeeuw CI, Wylie DR, DiGiorgi PL, Simpson JI (1994) Projections of individual Purkinje cells of identified zones in the flocculus to the vestibular and cerebellar nuclei in the rabbit. *J Comp Neurol* 349(3):428–447.
39. Nisimaru N, Okahara K, Yanai S (1998) Cerebellar control of the cardiovascular responses during postural changes in conscious rabbits. *Neurosci Res* 32(3):267–271.
40. Tsuchimochi H, Hayes SG, McCord JL, Kaufman MP (2009) Both central command and exercise pressor reflex activate cardiac sympathetic nerve activity in decerebrate cats. *Am J Physiol Heart Circ Physiol* 296(4):H1157–H1163.
41. Marcus JN, et al. (2001) Differential expression of orexin receptors 1 and 2 in the rat brain. *J Comp Neurol* 435(1):6–25.
42. Peyron C, et al. (1998) Neurons containing hypocretin (orexin) project to multiple neuronal systems. *J Neurosci* 18(23):9996–10015.
43. Marder E, Thirumalai V (2002) Cellular, synaptic and network effects of neuromodulation. *Neural Netw* 15(4-6):479–493.
44. Bester H, Besson JM, Bernard JF (1997) Organization of efferent projections from the parabrachial area to the hypothalamus: A *Phaseolus vulgaris*-leucoagglutinin study in the rat. *J Comp Neurol* 383(3):245–281.
45. Zhu Y, et al. (2003) Orexin receptor type-1 couples exclusively to pertussis toxin-insensitive G-proteins, while orexin receptor type-2 couples to both pertussis toxin-sensitive and -insensitive G-proteins. *J Pharmacol Sci* 92(3):259–266.
46. Eriksson KS, Sergeeva O, Brown RE, Haas HL (2001) Orexin/hypocretin excites the histaminergic neurons of the tuberomammillary nucleus. *J Neurosci* 21(23):9273–9279.
47. Murai Y, Akaike T (2005) Orexins cause depolarization via nonselective cationic and K+ channels in isolated locus coeruleus neurons. *Neurosci Res* 51(1):55–65.
48. Larsson KP, et al. (2005) Orexin-A-induced Ca2+ entry: Evidence for involvement of trpc channels and protein kinase C regulation. *J Biol Chem* 280(3):1771–1781.
49. Zhang J, et al. (2011) A role for orexin in central vestibular motor control. *Neuron* 69(4):793–804.
50. Rybicki KJ, Waldrop TG, Kaufman MP (1985) Increasing gracilis muscle interstitial potassium concentrations stimulate group III and IV afferents. *J Appl Physiol* 58(3):936–941.
51. Kumazawa T, Mizumura K (1977) Thin-fibre receptors responding to mechanical, chemical, and thermal stimulation in the skeletal muscle of the dog. *J Physiol* 273(1):179–194.